Magnetization-plateau state of the $S=3/2$ spin chain with single-ion anisotropy

Atsuhiro Kitazawa[1] and Kiyomi Okamoto[2]
[1]*Department of Physics, Kyushu University 33, Fukuoka 812-8581 Japan*
[2]*Department of Physics, Tokyo Institute of Technology, Oh-okayama, Meguro-ku, Tokyo 152-8551, Japan*
(Received 18 November 1999; revised manuscript received 29 March 2000)

We reexamine the numerical study of the magnetized state of the $S=3/2$ spin chain with single-ion anisotropy $D(>0)$ for the magnetization $M=M_S/3$, where M_S is the saturation magnetization. At this magnetization, we find that for $D<D_{c1}=0.387$ the system is critical and the magnetization plateau does not appear. For $D>D_{c1}$, the parameter region is divided into two parts $D_{c1}<D<D_{c2}=0.943$ and $D_{c2}<D$. In each region, the system is gapful and the $M=M_S/3$ magnetization plateau appears in the magnetization process. From our numerical calculation, the intermediate region $D_{c1}<D<D_{c2}$ should be characterized by a magnetized valence-bond-solid state.

I. INTRODUCTION

Recently, there has been a considerable interest in the magnetization process of one-dimensional quantum spin systems. Extending the Lieb-Schultz-Mattis theorem,[1] Oshikawa *et al.*[2] gave a necessary condition for the appearance of the magnetization plateau as $p(S-\langle m\rangle)=$integer, where S is the magnitude of the spin, p is the periodicity of the magnetic ground state in the thermodynamic limit, and $\langle m\rangle$ is the magnetization per site.

As a simple case, the $S=3/2$ spin chain with single-ion anisotropy (D) in a magnetic field h,

$$H=\sum_{j=1}^{L} \boldsymbol{S}_j\cdot\boldsymbol{S}_{j+1}+D\sum_{j=1}^{L}(S_j^z)^2-hM, \tag{1}$$

has been studied. Here $\boldsymbol{S}_j$ is the $S=3/2$ spin operator at the jth site, L is the system size, and M is the magnetization $M=\Sigma_j S_j^z$. Hereafter, we define the saturation magnetization as M_S $(=3L/2)$. In this model, a magnetization plateau can appear at $M=M_S/3$ $(p=1)$. For $D=0$ ($S=3/2$ Heisenberg model), a magnetization plateau does not appear.[3] On the other hand, for large D, the spin of each site tends to have $S^z=1/2$ for $M=M_S/3$, and a magnetization plateau appears. Oshikawa *et al.*[2] checked numerically that a magnetization plateau appears for $D=2$. Sakai and Takahashi[4] studied this model with the numerical diagonalization calculation using the phenomenological renormalization-group (PRG) analysis, and found that the transition point is $D_c=0.93\pm0.01$. They concluded that this point is the Berezinskii-Kosterlitz-Thouless (BKT) transition[5–7] point, that is, the plateau and the no-plateau transition point. Although the PRG analysis is a powerful method to study the second-order phase transition, this is not sufficient for the BKT transition because of the singular behavior of the energy gap and of the logarithmic size dependence of excitation energies. Thus, we think that it is worthwhile to reexamine this problem by use of another numerical approach.

The organization of this paper is as follows. In the next section, we consider an effective continuum model in order to investigate the mechanism of the appearance of the $M=M_S/3$ plateau. In Sec. III, we show the numerical method and the results with the numerical diagonalization data. To study the system, we first consider the finite-size behavior with conformal field theory and the renormalization-group analysis. Next, using them, we determine the boundary of the plateau and the no-plateau regions, and also check the critical behavior. The last section gives our conclusion.

II. EFFECTIVE CONTINUUM MODEL

For the magnetization $M=M_S/3$, the effective continuum model describing the low-energy physics is given by[2]

$$H_{\rm eff}=\int\frac{dx}{2\pi}\left[v_S K(\pi\Pi)^2+\frac{v_S}{K}\left(\frac{d\phi}{dx}\right)^2\right]+v_S y_\phi\int\frac{dx}{2\pi}\cos\sqrt{2}\phi, \tag{2}$$

where Π is the momentum density conjugate to ϕ, $[\phi(x),\Pi(x')]=i\delta(x-x')$, v_S is the sound velocity of the system. The dual field θ is defined as $\partial_x\theta=\pi\Pi$. The correlation exponents of several operators are governed by the coupling K and the scaling dimension of the operator $\sqrt{2}\cos\sqrt{2}\phi$ is $x=K/2$. Thus, the second term in the Hamiltonian (1) is relevant for $K<4$ and irrelevant for $K>4$.

The one-loop renormalization-group equations of this model are given by

$$\frac{dK(L)^{-1}}{d\ln L}=\frac{1}{8}y_\phi^2(L),\quad \frac{dy_\phi(L)}{d\ln L}=\left(2-\frac{K(L)}{2}\right)y_\phi(L),$$

where L is an infrared cutoff. These are the recursion relations of Kosterlitz.[7] The renormalization-group flow is shown in Fig. 1. In region A, the coupling K renormalized to a finite value and y_ϕ to zero; the system is critical and this corresponds to the no-plateau region in the spin system. In regions B and B', K renormalized to 0 and $|y_\phi|$ to ∞; these regions are massive phases and the field ϕ is locked to π and 0 for B and B' respectively. There is a separatrix $32K^{-1}-8\ln K^{-1}-y_\phi^2=8+8\ln 4$ that separates the infrared stable region (A) from the infrared unstable regions (B and B'). On this separatrix the BKT transition takes place. Near (K,y_ϕ)

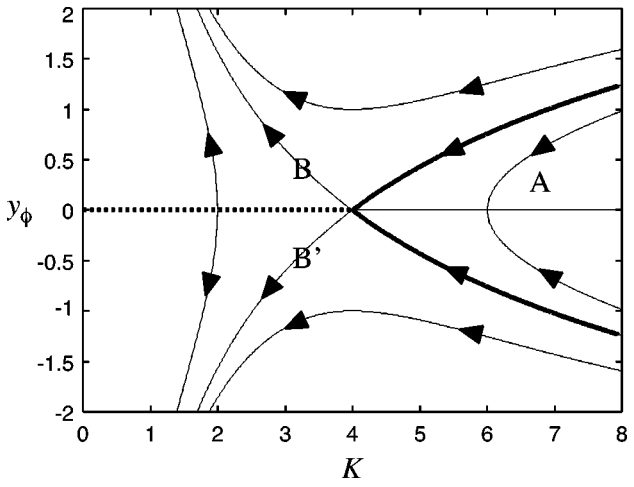

FIG. 1. Renormalization-group flow diagram. The bold lines (separating regions A and B, and A and B') are the BKT critical lines. On the dotted line between regions B and B' ($y_\phi=0, K<4$), a second-order phase transition occurs.

$=(4,0)$, and with the notation $K=4(1+y_0/2)$, the BKT transition point is on the line $|y_\phi|=y_0$, and we obtain

$$y_0(L)=\frac{y_0}{y_0\ln(L/L_0)+1}, \tag{3}$$

where y_0 and L_0 are the bare values, and y_0 flows to zero very slowly. Near the transition point and $y_0<|y_\phi|$, the energy gap—that is, the width of the plateau—behaves singularly as $\Delta h\sim\exp(-\text{const}/\sqrt{|y_\phi|-y_0})$.

According to the numerical calculation by Oshikawa *et al.*[2] for the $S=3/2$ Heisenberg chain ($D=0$) at the magnetization $M=M_S/3$, the Gaussian coupling K is $K\approx 4.4$, [in the notation of Ref. 2, the compactification radius is given by $R=(2\pi K)^{-1/2}=0.95/\sqrt{8\pi}$], and the system is gapless (no plateau). This value is slightly larger than the BKT critical (fixed point) coupling $K=4$.

III. NUMERICAL APPROACH AND RESULTS

A. Finite-size behavior

In order to study numerically, let us consider the finite-size behavior of the effective model (2) based on the conformal invariance.[8] The scaling dimension of the primary field $\mathcal{O}_{m,n}=\exp(im\sqrt{2}\phi+in\sqrt{2}\theta)$ for the fixed-point Hamiltonian ($y_\phi=0$) with the periodic boundary condition (PBC) is given by

$$x_{m,n}=\frac{K}{2}m^2+\frac{1}{2K}n^2, \tag{4}$$

where m and n are the ''magnetic'' and the ''electric'' charges in the Coulomb gas.[9] According to the conformal field theory, the state of the finite-size system has a correspondence to the operator in the infinite-size system, and the excitation energy of the finite-size system is given by

$$\Delta E_{m,n}(L)=E_{m,n}(L)-E_g(L)=\frac{2\pi v_S}{L}x_{m,n}, \tag{5}$$

where $E_g(L)$ is the ground-state energy of the L-site system with PBC.

The BKT transition takes place between the gapless and gapful regions, and the PRG analysis is affected by several irrelevant corrections sensitively. Moreover, on the transition point, there exists a logarithmic size correction in the excitation energy. PRG analysis does not suppose these features. In order to determine the BKT transition point, we apply the method proposed by Nomura and Kitazawa[10] (see also Refs. 11 and 12), which is free from the logarithmic size correction. If we can have the half-integer for the ''magnetic'' charge m, which is not permitted for PBC by the translational symmetry, we have the following finite-size spectrum for $m=\pm 1/2$:

$$x^c_{\pm 1/2,0}(L)\equiv\frac{L}{2\pi v_S}\Delta E^c_{\pm 1/2,0}(L)=\frac{K(L)}{8}+\frac{1}{2}y_\phi(L),$$

$$x^s_{\pm 1/2,0}(L)\equiv\frac{L}{2\pi v_S}\Delta E^s_{\pm 1/2,0}(L)=\frac{K(L)}{8}-\frac{1}{2}y_\phi(L), \tag{6}$$

where the energies $\Delta E^{c,s}_{\pm 1/2,0}(L)$ correspond to the operators $\sqrt{2}\cos\phi/\sqrt{2}$ and $\sqrt{2}\sin\phi/\sqrt{2}$, respectively. The term with y_ϕ comes from the first-order perturbation and from the operator product expansions,[13]

$$\sqrt{2}\cos\sqrt{2}\phi\left[\sqrt{2}\cos\frac{1}{\sqrt{2}}\phi\right]\sim\sqrt{2}\cos\frac{1}{\sqrt{2}}\phi,$$

$$\sqrt{2}\cos\sqrt{2}\phi\left[\sqrt{2}\sin\frac{1}{\sqrt{2}}\phi\right]\sim\sqrt{2}\sin\frac{1}{\sqrt{2}}\phi.$$

Near the BKT transition point $|y_\phi|=y_0$ [$K=4(1+y_0/2)$], defining $y_\phi=\pm y_0(1+t)$ where t measures the distance from the transition point, we have for $y_\phi>0$

$$x^c_{\pm 1/2,0}(L)=\frac{1}{2}+\frac{3}{4}y_0(L)\left(1+\frac{2}{3}t\right),$$

$$x^s_{\pm 1/2,0}(L)=\frac{1}{2}-\frac{1}{4}y_0(L)(1+2t), \tag{7}$$

and for $y_\phi<0$,

$$x^c_{\pm 1/2,0}(L)=\frac{1}{2}-\frac{1}{4}y_0(L)(1+2t),$$

$$x^s_{\pm 1/2,0}(L)=\frac{1}{2}+\frac{3}{4}y_0(L)\left(1+\frac{2}{3}t\right). \tag{8}$$

On the other hand, for $(m,n)=(0,\pm 2)$, corresponding to the operator $e^{\pm i2\sqrt{2}\theta}$, we have

$$x_{0,\pm 2}(L)\equiv\frac{L}{2\pi v_S}\Delta E_{0,\pm 2}(L)=\frac{2}{K}=\frac{1}{2}-\frac{1}{4}y_0(L). \tag{9}$$

In these scaling dimensions, the logarithmic size corrections are expressed by $y_0(L)$. From Eqs. (7), (8), and (9), energy differences $\Delta E^{s(c)}_{\pm 1/2,0}(L)$ and $\Delta E_{0,\pm 1}$ cross linearly at the BKT transition point $t=0$ for $y_\phi>0$ ($y_\phi<0$), and this behavior can be used to determine the BKT critical point.

From Eq. (6), $\Delta E^{c}_{\pm 1/2,0}$ and $\Delta E^{s}_{\pm 1/2,0}$ cross at $y_\phi = 0$.[13] This is the Gaussian fixed point. For $K<4$, the operator $\sqrt{2}\cos\sqrt{2}\phi$, which is in the second term of the Hamiltonian (2), is relevant and a second-order phase transition occurs at this point. On this transition point, we have $\Delta E^{c,s}_{\pm 1/2,0} < \Delta E_{0,\pm 2}$ from $K<4$.

The ''electric charge'' n in Eq. (5) relates to the variation of the magnetization from $M = M_S/3$, and the excitation energy $\Delta E_{0,\pm 2}$ in the spin system is described as

$$\Delta E_{0,\pm 2}(L) = \frac{E(M_S/3+2,L)+E(M_S/3-2,L)-2E(M_S/3,L)}{2}, \quad (10)$$

where $E(M,L)$ is the lowest energy for the magnetization M with the PBC. The excitation energies corresponding to the operator $\sqrt{2}\cos\phi/\sqrt{2}$ and $\sqrt{2}\sin\phi/\sqrt{2}$ are obtained by the two low energies with the twisted boundary condition (TBC) (Refs. 17–20) $S^{\pm}_{L+1} = -S^{\pm}_{1}$, $S^{z}_{L+1} = S^{z}_{1}$ as

$$\Delta E^{c}_{\pm 1/2,0}(L) = E^{\mathrm{TBC}}(M_S/3,L,1) - E(M_S/3,L), \quad (11)$$

$$\Delta E^{s}_{\pm 1/2,0}(L) = E^{\mathrm{TBC}}(M_S/3,L,-1) - E(M_S/3,L),$$

where $E^{\mathrm{TBC}}(M_S/3,L,P)$ is the lowest energy with the magnetization $M = M_S/3$ and with the parity P: $\boldsymbol{S}_j \to \boldsymbol{S}_{L-j+1}$.

B. Numerical results

Here, we show our numerical results. We calculate the energy of finite-size systems $L = 8$, 10, 12, 14 with the numerical diagonalization calculation. In the region $D>0$, the lowest energy state with the magnetization M and with PBC has the parity $P = (-1)^{M+L/2}$ and the momentum $q = (M + L/2)\times\pi$.

Figure 2(a) shows the energy differences $\Delta E^{c}_{\pm 1/2,0}$, $\Delta E^{s}_{\pm 1/2,0}$, and $\Delta E_{0,\pm 2}$ for $L = 14$ systems. We find that among these three energies the lowest one is $\Delta E_{0,\pm 2}$ for small $D(0<D<D_{c_1})$ and $\Delta E^{c}_{\pm 1/2,0}$ for large $D(D_{c2}<D)$. In the intermediate region $D_{c1}<D<D_{c2}$, $\Delta E^{s}_{\pm 1/2,0}$ is lower than $\Delta E^{c}_{\pm 1/2,0}$ and $\Delta E_{0,\pm 2}$. In Fig. 1, the small D region $0 < D < D_{c1}$ should correspond to region A, the intermediate region $D_{c1}<D<D_{c2}$ to B, and the large D region to B'.

From the critical properties of the effective model (2) [see Eqs. (7) and (9)], the point D_{c1} should be a BKT critical point. The size dependence of the crossing points between $\Delta E^{s}_{\pm 1/2,0}$ and $\Delta E_{0,\pm 2}$ is shown in Fig. 3(a) and the extrapolated value is given by $D_{c1} = 0.387$. For small $D(<D_{c1})$, the excitation spectrum is gapless and there does not exist a plateau in the magnetization curve.

In order to check this, we calculate the averaged scaling dimension,[10–12]

$$[x^{c}_{\pm 1/2,0}(L) + 3x^{s}_{\pm 1/2,0}(L)]/4, \quad (12)$$

at the point $D = D_{c1}$. From Eq. (7), this value cancels the leading logarithmic size correction, and should be 1/2 at $D = D_{c1}$. To calculate the scaling dimension, we need the sound velocity v_S. This can be calculated using the lowest energy with $M = M_S/3$ and the wave number $q = 2\pi/L$ [corresponding to the U(1) current],

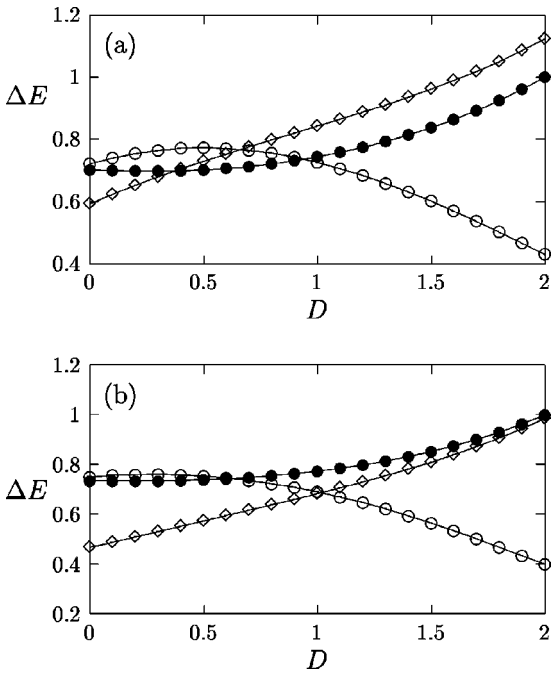

FIG. 2. (a) Energy differences $\Delta E^{c}_{\pm 1/2,0}$ (○), $\Delta E^{s}_{\pm 1/2,0}$ (●), and $\Delta E_{0,\pm 2}$ (◇) for the system (1) with $L = 14$. The crossing point of $\Delta E^{s}_{\pm 1/2,0}$ and $\Delta E_{0,\pm 2}$ is the BKT critical point. The crossing point of $\Delta E^{c}_{\pm 1/2,0}$ and $\Delta E^{s}_{\pm 1/2,0}$ is a second-order phase transition point. (b) Energy differences $\Delta E^{c}_{\pm 1/2,0}$ (○), $\Delta E^{s}_{\pm 1/2,0}$ (●), and $\Delta E_{0,\pm 2}$ (◇) for the system (20) with $\Delta = 0.5$ and $L = 14$. The crossing point of $\Delta E^{c}_{\pm 1/2,0}$ and $\Delta E_{0,\pm 2}$ is the boundary between the no-plateau and the large-D regions. The crossing point of $\Delta E^{c}_{\pm 1/2,0}$ and $\Delta E^{s}_{\pm 1/2,0}$ is the Gaussian fixed point in the no-plateau region.

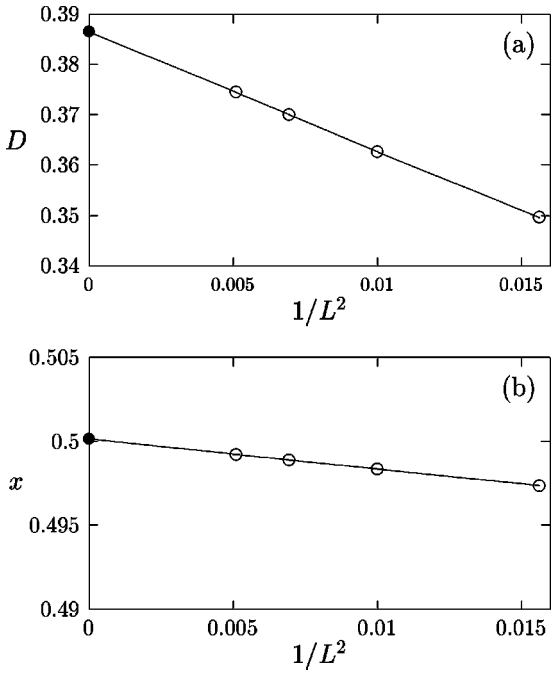

FIG. 3. (a) Size dependence of the crossing point between the energy differences $\Delta E^{s}_{\pm 1/2,0}$ and $\Delta E_{0,\pm 2}$. The BKT critical point is estimated as $D_{c1} = 0.387$. (b) Size dependence of the averaged scaling dimension $(x^{c}_{\pm 1/2,0} + 3x^{s}_{\pm 1/2,0})/4$ at the BKT critical point $D_{c1} = 0.387$.

$$v_S(L)=\frac{E(M_S/3,L,q=2\pi/L)-E(M_S/3,L)}{2\pi/L}. \quad (13)$$

We extrapolate this finite-size value in the polynomial of $1/L^2$, and obtain $2\pi v_S=20.06$. Figure 3(b) shows the size dependence of the value (12). We can see that the extrapolated value is very close to the expected one 1/2. L^{-2} correction comes from irrelevant operators with scaling dimension $x=4$.[8] We also calculate the conformal anomaly number c from

$$\frac{E(M_S/3,L)}{L}=\epsilon_{\langle m\rangle=1/2}-\frac{\pi v_S c}{6L^2}+\cdots, \quad (14)$$

where $\epsilon_{\langle m\rangle=1/2}$ is the energy per site of the limit $L\to\infty$, c is the conformal anomaly number, and $\cdots$ means the higher-order size correction. We estimate c at $D=D_{c1}$ as $c=0.97$, which is close to the expected value $c=1$.

Thus, we can conclude that the point $D=D_{c1}$ is the BKT critical point. The width of the plateau near the transition point behaves as $\Delta h\sim\exp(-\text{const}/\sqrt{D-D_{c1}})$.

According to Eq. (6), the crossing point D_{c2} between $\Delta E^c_{\pm 1/2,0}$ and $\Delta E^s_{\pm 1/2,0}$ should be a second-order phase transition point ($K<4$ and $y_\phi=0$). For large $D(D_{c2}<D)$, the system is in the large-D region and a plateau appears in the magnetization curve at $M=M_S/3$. Thus, we have another massive phase in the region $D_{c1}<D<D_{c2}$. As a possibility, this intermediate region should be characterized by the following partially magnetized valence-bond-solid (VBS) state:

$$|\psi^{(\mathrm{PBC})}_{\mathrm{mVBS}}\rangle=a^\dagger_L(a^\dagger_L b^\dagger_1-b^\dagger_L a^\dagger_1)| \times\prod_{j=1}^{L-1} a^\dagger_j(a^\dagger_j b^\dagger_{j+1}-b^\dagger_j a^\dagger_{j+1})|0\rangle, \quad (15)$$

where we describe the spin state by the Schwinger bosons, that is, $a^\dagger_j$ ($b^\dagger_j$) creates the $S=1/2$ $\uparrow(\downarrow)$ spin at the jth site, and $|0\rangle$ is the vacuum of the Schwinger bosons. Here we assume PBC. This partially magnetized VBS state had been discussed by Oshikawa[21] for another model (see also Ref. 2).

Let us consider the crossing behavior near the point $D=D_{c2}$ on this point of view. The large-D phase is characterized by the state

$$|\psi_{\text{large }D}\rangle=\prod_{j=1}^{L} a^\dagger_j(a^\dagger_j b^\dagger_j)|0\rangle. \quad (16)$$

With the twisted boundary condition ($a^\dagger_{L+1}=a^\dagger_1, b^\dagger_{L+1}=-b^\dagger_1$), the magnetized valence-bond-solid state is described as

$$|\psi^{(\mathrm{TBC})}_{\mathrm{mVBS}}\rangle=a^\dagger_L(a^\dagger_L b^\dagger_1+b^\dagger_L a^\dagger_1) \times\prod_{j=1}^{L-1} a^\dagger_j(a^\dagger_j b^\dagger_{j+1}-b^\dagger_j a^\dagger_{j+1})|0\rangle, \quad (17)$$

while the large-D state is also characterized by Eq. (16). The state $|\psi^{(\mathrm{TBC})}_{\mathrm{mVBS}}\rangle$ has the parity of the space inversion $P=-1$, while the large-D state has $P=1$. This explains the level crossing between $\Delta E^c_{\pm 1/2,0}$ and $\Delta E^s_{\pm 1/2,0}$ in Fig. 2(a).

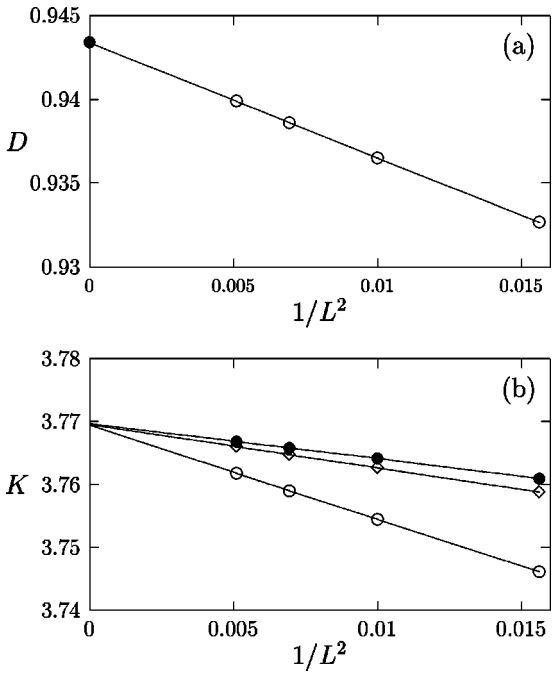

FIG. 4. (a) Size dependence of the crossing point between the energy differences $\Delta E^c_{\pm 1/2,0}$ and $\Delta E^s_{\pm 1/2,0}$. The critical point between the intermediate and the magnetic large-D regions is estimated as $D_{c2}=0.943$. (b) Parameter K obtained by the data $x^c_{\pm 1/2,0}=K/8$ (○), $x^s_{\pm 1/2,0}=K/8$ (●), and $x_{0,\pm 1}=1/2K$ (◇). The extrapolated value is $K=3.77$.

The size dependence of the crossing point is shown in Fig. 4(a). The estimated critical point between the intermediate and the large-D regions is $D_{c2}=0.943$, which is very close to the value $D_c=0.93\pm 0.01$ obtained by Sakai and Takahashi. However, the phase transition is not of the BKT type but a second-order phase transition that is the same universality class as the Haldane–large-D transition in the $S=1$ anisotropic model,[14–16]

$$H_{S=1}=\sum_{j=1}^{L}[S^x_jS^x_{j+1}+S^y_jS^y_{j+1}+\Delta S^z_jS^z_{j+1}]+D\sum_{j=1}^{L}(S^z_j)^2. \quad (18)$$

Especially, the intermediate region of the model (1) corresponds to the $S=1$ Haldane phase in Eq. (18).

To verify that the point $D=D_{c2}$ is a second-order phase transition point, we calculate the coupling K. The sound velocity is evaluated as $2\pi v_S=21.87$. Using this value, we determine K from $x^s_{\pm 1/2,0}(L)$, $x^c_{\pm 1/2,0}(L)$ [Eqs. (6) ($y_\phi=0$)], and

$$\frac{L}{2\pi v_S}\Delta E_{0,\pm 1}(L)=x_{0,\pm 1}(L)=1/2K, \quad (19)$$

$$\Delta E_{0,\pm 1}(L)=\frac{E(M_S/3+1,L)+E(M_S/3-1,L)-2E(M_S/3,L)}{2},$$

as shown in Fig. 4(b). Extrapolated values of these three are consistent, and we obtain $K=3.77$. This is smaller than the BKT fixed-point value, and the point $D=D_{c2}$ should be a

second-order phase transition point. We also estimate the conformal anomaly number from Eq. (14), and check that it is very close to the expected value $c=1$.

In the vicinity of the critical point $D=D_{c2}$, the width of the magnetization plateau decreases as $\Delta h \sim |D-D_{c2}|^{\nu}$, where the critical exponent ν is given by $\nu=1/(2-x_{\pm 1,0})=8.68$

Restricting to three states $S^z=3/2$, 1/2, and $-1/2$ (in sufficiently large magnetic field) Sakai and Takahashi mapped the $S=3/2$ model to an $S=1$ generalized anisotropic model with $h=0$. In order to investigate the relation between the $S=1$ with $h=0$ and the $S=3/2$ model in a magnetic field, we further applied the same analysis to the following $S=3/2$ model:

$$H_{\Delta}=\sum_{j}^{L}\ (S_j^x S_{j+1}^x+S_j^y S_{j+1}^y+\Delta S_j^z S_{j+1}^z)$$

$$+D\sum_{j}^{L}\ (S_j^z)^2-h\sum_{j}^{L}\ S_j^z, \qquad (20)$$

in the region $0\leqslant\Delta\leqslant 1$. Figure 2(b) shows the energy differences $\Delta E^{c}_{\pm 1/2,0}$, $\Delta E^{s}_{\pm 1/2,0}$, and $\Delta E_{0,\pm 2}$ for $L=14$, $\Delta=0.5$ system. The lowest one is $\Delta E_{0,\pm 2}$ for small D and $\Delta E^{c}_{\pm 1/2,0}$ for large D. In this case, there is a BKT transition between the no-plateau and the large-D regions. [The crossing point of $\Delta E^{c}_{\pm 1/2,0}$ and $\Delta E^{s}_{\pm 1/2,0}$ is the Gaussian fixed point $y_{\phi}=0$ in the no-plateau region $(K>4)$.]

We show the Δ-D diagram in Fig. 5. We found that for $0.808<\Delta<1$, the $M=M_S/3$ phase structure is the same as that of the $\Delta=1$ case, and there exists the intermediate magnetic region $(D_{c1}<D<D_{c2})$. But for $0<\Delta<0.808$, the direct transition (BKT type) occurs between the no-plateau and the large-D regions. This boundary runs from $(\Delta,D)=(0,1.312)$ to the multicritical point (0.808,0.817). The phase structure is topologically the same as that of the $S=1$ anisotropic model[14–16] with $h=0$ (18).

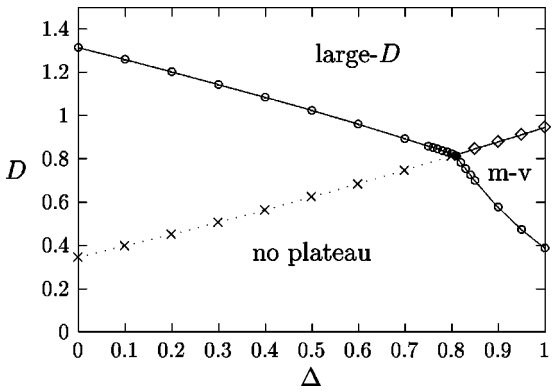

FIG. 5. The boundary of the no-plateau, the large-D, and the magnetized VBS (m-v) regions. The boundary between the no-plateau and the large-D regions, and between the no-plateau and the magnetized VBS regions (○) are the BKT critical lines. The boundary between the large-D and the magnetized VBS regions (◇) is a second-order critical line. The multicritical point of these regions (●) are estimated as $(\Delta,D)=(0.808,0.817)$. We also show the Gaussian fixed line in the no-plateau region (×).

IV. CONCLUSION

We studied the $S=3/2$ spin chain with the single-ion anisotropy in a magnetic field (1). With the numerical approach based on the field theoretical analysis, we determined boundaries between the plateau and the no-plateau regions and found an intermediate plateau-region between the no-plateau $(D<D_{c1}=0.387)$ and the magnetized large-D $(D_{c2}=0.943<D)$ regions. In order to check the critical properties, we estimated the conformal anomaly number, the averaged scaling dimension [Fig. 3(b)], and the Gaussian coupling [Fig. 4(b)], and obtained consistent results with the argument in Sec. III A. As far as we know, this is the first work in which a no-plateau state and two kinds of plateau states are found when the parameter is changed in a simple and realistic model. This intermediate region should have the same character of the partially magnetized valence-bond-solid state, and should be characterized by the string order parameter[21–23] and by the edge states for the open boundary system[24,25] reflecting a hidden discrete symmetry.[21,26] But in our small-size calculation, we could not collect this evidence, because the critical exponent $\nu=8.68$ at $D=D_{c2}$ is somewhat large, and it is expected that the correlation length is large in the intermediate region.

We also studied the model with the exchange (Δ) and the on-site (D) anisotropies (20). In this case, we found that for $\Delta<0.808$, the intermediate region that exists for the $\Delta=1$ case disappears. The boundaries of the plateau and the no-plateau regions are the same as Fig. 1 and the $S=1$ anisotropic model (18).

ACKNOWLEDGMENTS

We acknowledge K. Nomura, M. Oshikawa, and T. Sakai for discussions. The computation in this work was performed using the facilities of the Supercomputer Center, Institute for Solid State Physics, University of Tokyo.

[1] E. Lieb, T.D. Schultz, and D.C. Mattis, Ann. Phys. (N.Y.) **16**, 407 (1961).
[2] M. Oshikawa, M. Yamanaka, and I. Affleck, Phys. Rev. Lett. **78**, 1984 (1997).
[3] J.B. Parkinson and J.C. Bonner, Phys. Rev. B **32**, 4703 (1985).
[4] T. Sakai and M. Takahashi, Phys. Rev. B **57**, R3201 (1998).
[5] V.L. Berezinskii, Zh. Éksp. Teor. Fiz. **59**, 907 (1970) [Sov. Phys. JETP **32**, 493 (1971)]; **61** 1144 (1971) [**34**, 610 (1971)].
[6] J.M. Kosterlitz and D.J. Thouless, J. Phys. C **6**, 1181 (1973).
[7] J.M. Kosterlitz, J. Phys. C **7**, 1046 (1974).
[8] J. Cardy, J. Phys. A **17**, L385 (1984); Nucl. Phys. B: Field Theory Stat. Syst. **270** [FS16], 186 (1986).
[9] L.P. Kadanoff, J. Phys. A **11**, 1399 (1978).
[10] K. Nomura and A. Kitazawa, J. Phys. A **31**, 7341 (1998).

[11] K. Okamoto and A. Kitazawa, J. Phys. A **32**, 4601 (1999).
[12] A. Kitazawa and K. Okamoto, J. Phys.: Condens. Matter **11**, 9765 (1999).
[13] A. Kitazawa, J. Phys. A **30**, L285 (1997).
[14] R. Botet, R. Jullien, and M. Kolb, Phys. Rev. B **28**, 3914 (1983).
[15] J. Sólyom and T.A.L. Ziman, Phys. Rev. B **30**, 3980 (1984).
[16] H. Schulz and T. Ziman, Phys. Rev. B **33**, 6545 (1986).
[17] H.W.J. Blöte, J.L. Cardy, and M.P. Nightingale, Phys. Rev. Lett. **56**, 742 (1986).
[18] F.C. Alcaraz, M.N. Barber, and M.T. Batchelor, Phys. Rev. Lett. **58**, 771 (1987); Ann. Phys. (N.Y.) **182**, 280 (1988).
[19] C. Destri and H.J. de Vega, Phys. Lett. B **223**, 365 (1989).
[20] T. Fukui and N. Kawakami, J. Phys. Soc. Jpn. **65**, 2824 (1996).
[21] M. Oshikawa, J. Phys.: Condens. Matter **4**, 7469 (1992).
[22] M. den Nijs and K. Rommelse, Phys. Rev. B **40**, 4709 (1989).
[23] H. Tasaki, Phys. Rev. Lett. **66**, 798 (1991).
[24] I. Affleck, T. Kennedy, E. Lieb, and H. Tasaki, Phys. Rev. Lett. **59**, 799 (1987); Commun. Math. Phys. **115**, 477 (1988).
[25] T. Kennedy, J. Phys.: Condens. Matter **2**, 5737 (1990).
[26] T. Kennedy and H. Tasaki, Phys. Rev. B **45**, 304 (1992); Commun. Math. Phys. **147**, 431 (1992).